Title

Estimating patient dose from CT exams that use automatic exposure control: Development and validation of methods to accurately estimate tube current values.

Journal

Medical Physics, 44(8)

Authors

McMillan, Kyle
Bostani, Maryam
Cagnon, Christopher
et al.

Publication Date

2017-08-01

DOI

10.1002/mp.12314

Peer reviewed

Estimating patient dose from CT exams that use automatic exposure control: Development and validation of methods to accurately estimate tube current values

Kyle McMillan
Biomedical Physics, David Geffen School of Medicine, University of California, Los Angeles, Los Angeles, CA 90024, USA
Department of Radiology, Mayo Clinic, Rochester, MN 55905, USA

Maryam Bostani and Christopher H. Cagnon
Biomedical Physics, David Geffen School of Medicine, University of California, Los Angeles, Los Angeles, CA 90024, USA
Department of Radiological Sciences, David Geffen School of Medicine, University of California, Los Angeles, Los Angeles, CA 90024, USA

Lifeng Yu, Shuai Leng, and Cynthia H. McCollough
Department of Radiology, Mayo Clinic, Rochester, MN 55905, USA

Michael F. McNitt-Gray[a)]
Biomedical Physics, David Geffen School of Medicine, University of California, Los Angeles, Los Angeles, CA 90024, USA
Department of Radiological Sciences, David Geffen School of Medicine, University of California, Los Angeles, Los Angeles, CA 90024, USA

(Received 29 August 2016; revised 4 April 2017; accepted for publication 9 April 2017; published 30 June 2017)

Purpose: The vast majority of body CT exams are performed with automatic exposure control (AEC), which adapts the mean tube current to the patient size and modulates the tube current either angularly, longitudinally or both. However, most radiation dose estimation tools are based on fixed tube current scans. Accurate estimates of patient dose from AEC scans require knowledge of the tube current values, which is usually unavailable. The purpose of this work was to develop and validate methods to accurately estimate the tube current values prescribed by one manufacturer's AEC system to enable accurate estimates of patient dose.

Methods: Methods were developed that took into account available patient attenuation information, user selected image quality reference parameters and x-ray system limits to estimate tube current values for patient scans. Methods consistent with AAPM Report 220 were developed that used patient attenuation data that were: (a) supplied by the manufacturer in the CT localizer radiograph and (b) based on a simulated CT localizer radiograph derived from image data. For comparison, actual tube current values were extracted from the projection data of each patient. Validation of each approach was based on data collected from 40 pediatric and adult patients who received clinically indicated chest (n = 20) and abdomen/pelvis (n = 20) scans on a 64 slice multidetector row CT (Sensation 64, Siemens Healthcare, Forchheim, Germany). For each patient dataset, the following were collected with Institutional Review Board (IRB) approval: (a) projection data containing actual tube current values at each projection view, (b) CT localizer radiograph (topogram) and (c) reconstructed image data. Tube current values were estimated based on the actual topogram (actual-topo) as well as the simulated topogram based on image data (sim-topo). Each of these was compared to the actual tube current values from the patient scan. In addition, to assess the accuracy of each method in estimating patient organ doses, Monte Carlo simulations were performed by creating voxelized models of each patient, identifying key organs and incorporating tube current values into the simulations to estimate dose to the lungs and breasts (females only) for chest scans and the liver, kidney, and spleen for abdomen/pelvis scans. Organ doses from simulations using the actual tube current values were compared to those using each of the estimated tube current values (actual-topo and sim-topo).

Results: When compared to the actual tube current values, the average error for tube current values estimated from the actual topogram (actual-topo) and simulated topogram (sim-topo) was 3.9% and 5.8% respectively. For Monte Carlo simulations of chest CT exams using the actual tube current values and estimated tube current values (based on the actual-topo and sim-topo methods), the average differences for lung and breast doses ranged from 3.4% to 6.6%. For abdomen/pelvis exams, the average differences for liver, kidney, and spleen doses ranged from 4.2% to 5.3%.

Conclusions: Strong agreement between organ doses estimated using actual and estimated tube current values provides validation of both methods for estimating tube current values based on data provided in the topogram or simulated from image data. [https://doi.org/10.1002/mp.12314]

Key words: computed tomography, Monte Carlo simulations, organ dose, radiation dose, tube current modulation

1. INTRODUCTION

In current clinical practice, most CT exams are performed with automatic exposure control (AEC), a technique that adjusts tube current according to changes in patient attenuation.[1] Studies have shown AEC systems to reduce mean scanner output (tube current–time product) as much as 91% when compared with fixed tube current (FTC) acquisitions.[2,3] The potentially large discrepancies between tube current values from AEC and FTC scans highlight the need to incorporate AEC behaviors into dose estimation tools to ensure an accurate representation of actual patient dose (and the actual dose savings from the use of AEC).

Monte Carlo simulations of CT examinations using AEC can be performed using tube current values extracted from the projection data of patients who underwent actual CT examinations.[4,5] These schemes are the actual tube current profiles (tube current as a function of tube angle and table position) generated for a given patient's anatomy, and therefore, organ doses estimated using these tube current values can be considered to be accurate estimates of the true organ dose for an AEC CT examination ("reference standard"). When the projection data are not available, Khatonabadi et al. described a method to use the tube current profile extracted from a patient's axial images (tube current as a function of table position only) as a surrogate for the complete tube current profile extracted from the projection data.[6] For either scenario, organ dose estimates are limited to fully irradiated organs that can be observed and easily segmented from the CT image data. Doses to partially and indirectly irradiated organs cannot be estimated because they are not fully contained within the image volume. Without this dose information, dose metrics that require the knowledge of dose to all radiosensitive organs, such as effective dose, cannot be directly estimated (they would require assumptions about organ placement, organ and patient size, and organ distance from the irradiated, volume as well as assumptions about the tube current behavior).

One way to determine the radiation dose to any fully-, partially- or indirectly irradiated organ for any CT exam performed with AEC is to simulate AEC CT exams for reference voxelized phantoms of various sizes that have all radiosensitive organs identified, such as the GSF and International Commission on Radiological Protection (ICRP) reference voxelized phantoms.[7,8] This would allow for the identification of relationships between patient size and organ doses, similar to those observed for FTC as described in AAPM Report 204.[9] This would also allow for the estimation of other dose/risk descriptors, such as effective dose, as a function of patient size. These methods could be integrated into large scale epidemiology studies that seek to correlate stochastic effects with patient dose.

However, there are no validated tube current profiles for these reference voxelized phantoms. Early efforts to model tube current behavior concentrated on the development of idealized, attenuation-based tube current profiles.[10,11] These theoretical models were later incorporated into Monte Carlo simulations to estimate organ dose from AEC CT examinations.[12–15] Even though AEC algorithms for each major CT manufacturer are based on the general idea that tube current will be adjusted in response to changes in patient attenuation, they differ substantially in implementation. Thus, the major limitation of models of idealized tube current profiles is that they do not represent any manufacturer-specific AEC system.[16] Specific issues such as x-ray tube and generator limits imposed by the scanner and scanner-specific modulation schemes (e.g., on-line modulation) are not explicitly modeled in these approaches. Therefore, organ doses estimated using these idealized tube current behaviors are also idealized; they are not necessarily the organ doses the reference voxelized phantoms would have received had they been scanned on an actual CT scanner with an actual AEC system. Clearly, Monte Carlo simulations that incorporate the behavior of realistic AEC systems are needed. This requires methods to accurately predict the realistic tube current values that would have occurred if these patient models had undergone an AEC CT exam.

Therefore, the purpose of this investigation was to develop and validate methods to estimate scanner-specific tube current values for any voxelized patient model. This work specifically developed methods that take into account patient attenuation information, scanner tube, and generator limits and user-selected parameters so that realistic tube current profiles can be generated and accurate estimates of patient dose can be calculated.

This manuscript describes methods to estimate tube current values based on the AEC algorfithm from one manufacturer (CARE Dose4D, Siemens Healthcare, Forchheim, Germany). This AEC algorithm adjusts scanner output across different body regions (i.e., different attenuations) according to the prescribed reference image quality; it does not attempt to keep the noise constant across patient size or body region.[17] The algorithm also automatically adjusts tube current to the size and shape of the patient through both longitudinal and angular modulation. Patient attenuation data used to drive the algorithm can be extracted from the CT localizer radiograph (i.e., topogram) [18] and is consistent with the data requested from manufacturers by AAPM Report 220.[19] Alternatively, the patient attenuation data can be obtained based on a simulated topogram using methods described herein. This work describes both methods for estimating the tube current values. It also describes experiments carried out to validate each approach by comparing estimated and actual tube current values for patient scans, as well as associated organ dose estimates.

2. MATERIALS AND METHODS

The first method for obtaining patient attenuation information is direct extraction from the CT localizer radiograph, when it is available. The second method is developed for situations where the CT localizer radiograph is not available (such as when using a reference voxelized patient model). This latter method involves simulating the topogram and applying a series of calculations and adjustments to emulate what the manufacturer does to derive the attenuation data. After patient attenuation data are obtained, tube current values are then predicted from this attenuation data. Evaluation of the described methods were made using actual patient scan data to: (a) directly compare the estimated and actual tube current values from these scans and (b) compare estimates of organ dose from Monte Carlo simulations using the estimated and actual tube current values.

2.A. Size data from actual CT scan localizer radiograph

Before CT images are acquired, a CT localizer radiograph is obtained. This projection image aids in aligning the patient and setting the appropriate scan range. Based on the scanner manufacturer and the scan protocol, an anterior-posterior (AP) radiograph, lateral (LAT) radiograph, or both are acquired. Patient attenuation data are derived from these projection images and are used with all AEC algorithms, which require knowledge of patient attenuation.[2] Within the DICOM header of a Siemens topogram, there exists a private field that contains the words "ATTENUATION" and "AEC" within the description of the field and its subfields. Within one of the subfields, an array of numbers equal to two times the length of the topogram exists. These data are the AP and LAT water-equivalent estimates of patient size.[18] These data were available in the CT scanners used in this work for software versions VA40 and later (up to VA44 to date). Figure 1 shows an example of the AP and LAT water-equivalent estimates (length of water path with the same attenuation) of patient size extracted from the topogram of an adult patient. The patient size data were extracted directly from the DICOM header of the topogram without further calculation. This chest CT from an adult patient will be used as an example throughout the methods section.

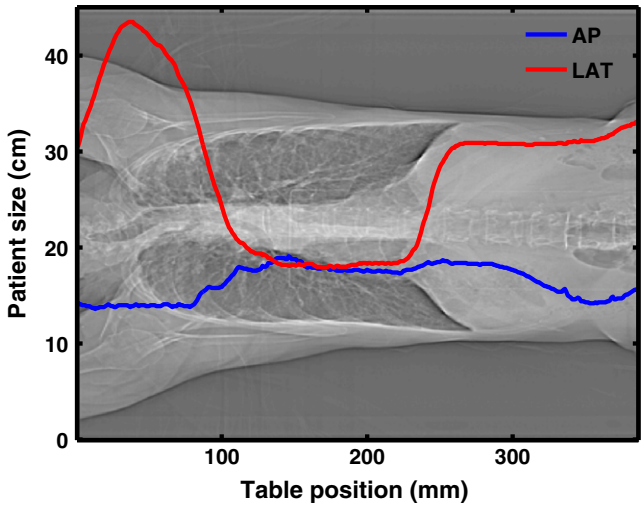

FIG. 1. AP and LAT water-equivalent estimates of patient size extracted from the DICOM header of a topogram. [Color figure can be viewed at wileyonlinelibrary.com]

2.B. Size data from simulated CT localizer radiograph

2.B.1. Creating a simulated CT scan localizer radiograph

In situations where a CT scan localizer radiograph is not available, a method is needed to simulate one so that the patient attenuation information described above can be estimated. Patient attenuation was modeled in this investigation using Monte Carlo simulations, which included the detailed equivalent source model of the x-ray source and bowtie filtration as described previously,[20] to model the projection geometry of the topogram. Because an AP topogram is typically acquired for all body scans (e.g., chest and abdomen/pelvis scans), the geometry for AP radiographic imaging was modeled. The CT source was fixed at the 12 o'clock position (i.e., directly above the patient) at the source-to-isocenter distance (SID) of the scanner of interest. A linear detector array consisting of 100 1-cm × 1-cm detector elements was modeled at the source-to-detector distance (SDD) for the scanner of interest. A linear detector was modeled for simplicity, even though it is recognized that the actual detector design for most CT scanners has some curvature. In this investigation, simulations were performed using an equivalent source model based on a 64 slice multidetector CT (Sensation 64, Siemens Healthcare, Forchheim, Germany),[20] which accounts for the polychromatic beam spectrum and the effects of the bowtie filter. For this scanner, the SID and SDD are 57 cm and 104 cm respectively. A narrow beam collimation of 6 × 0.6 mm (3.6 mm) was used. This is the collimation used when a topogram is acquired on the scanner. All simulations were performed with a tube potential of 120 kV.

After the simulation geometry was set up, an "air scan" was performed. This determined the intensity of the x-ray beam at the detector with no object in the scanner. With no object or table present in the simulation, photon fluence (#/cm^2/particle) was tallied at each detector element. Per particle photon fluence is the direct output of the Monte Carlo simulations. This simulation only needed to be performed once for the evaluated scanner model. Then, a "patient scan" was performed. This determined the intensity of the x-ray beam at the detector with the object in the scanner. With the object present, photon fluence was again tallied at each detector element. Patient scans were performed in 1 mm increments along the length of the object. Figure 2 (left) shows an example of the fluence profiles along the detector from the air and patient scans at a particular table location for an adult patient who underwent a clinically indicated chest CT exam (same

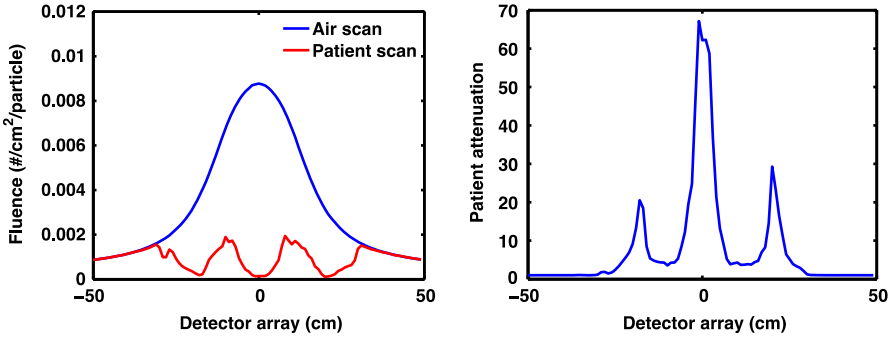

FIG. 2. (Left) Air scan and patient scan fluence profiles at a particular table location. (Right) Patient attenuation profile along the detector calculated by dividing the fluence profile from the air scan by the fluence profile from the patient scan. [Color figure can be viewed at wileyonlinelibrary.com]

patient as in Fig. 1). Patient attenuation along the detector was calculated at each table position by dividing the fluence profile from the air scan by the fluence profile from the patient scan. Figure 2 (right) shows the patient attenuation profile along the detector calculated from the fluence profiles. The determination of patient attenuation profiles at each table location is analogous to simulating an AP topogram.

2.B.2. Anterior-posterior dimension of patient size

From the patient attenuation profile at each table location, the AP patient dimension was calculated at each table location. To eliminate the influence of strong local attenuations, such as metallic implants, screws or clips, on the calculation of AP size, a moving average filter was first applied to the attenuation profile.[21] The span of the moving average corresponds to 5 of the 1 cm detector elements (5 cm total) as described above in Section 2.B.1 and illustrated in Fig. 3. After the filter was applied, the maximum attenuation from the profile was determined. The AP patient dimension calculated from the maximum attenuation of the attenuation profile at each table position, was defined as:

$$AP(i) = \frac{1}{\mu_{water,E}} \times \ln(\max(A(i))) \quad (1)$$

where $\mu_{water,E}$ is the linear attenuation coefficient of water for a given beam energy and $A(i)$ is the filtered attenuation profile.[22] As mentioned in Section 2.B.1, all simulations were performed using a 120 kV spectra, which was determined to an effective energy of approximately 60 keV when performing the measurements required to create the equivalent source as described in.[20] Therefore, $\mu_{water,E} = \mu_{water,60keV} = 0.2\text{cm}^{-1}$.

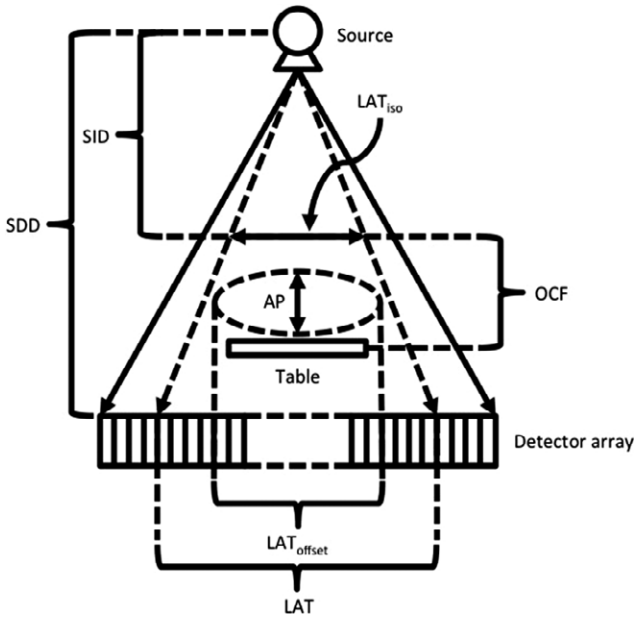

FIG. 3. Diagram of scanner geometry with all components of Eq. 4 labeled.

2.B.3. Lateral dimension of patient size

To emulate the Siemens AEC algorithm, patient attenuation data in the AP direction, derived from the simulated AP topograms described above, were utilized to estimate the LAT patient dimension using a mathematical model.[22] This mathematical model involves the elimination of outside air, the CT table and low-attenuation regions through the application of thresholds to the patient attenuation profile.[21] An initial estimate of the LAT patient dimension was calculated by multiplying the number of detector elements with attenuations greater than the thresholds by the detector element width.[21] The initial estimate of lateral dimension at each table position, i, was defined as:

$$LAT(i) = n\{A(i)|A(i) > t_{air,table}, t_{low-attenuation}\} \times w_d \quad (2)$$

where $t_{air,table}$ is the threshold for outside air and the table, $t_{low-attenuation}$ is the threshold for low-attenuation regions, $n\{A(i)|A(i) > t_{air,table}, t_{low-attenuation}\}$ is the number of detector elements with attenuations greater than the thresholds and w_d is the detector element width. In this work, w_d was 1 cm, $t_{air,table}$ was 1.4 (arbitrary units) and $t_{low-attenuation}$ was set as 9% of the maximum attenuation of the attenuation profile.

This initial estimate of lateral patient dimension was based on the "shadow" of the patient on the detector array and therefore needs to be geometrically corrected to the position of the patient within the CT scanner.[22] An estimate of lateral

patient dimension at the scanner isocenter at each table position, i, was defined as:

$$LAT(i)_{iso} = \frac{SID}{SDD} \times LAT(i) \tag{3}$$

If the patient was perfectly aligned at isocenter, this would be the true lateral dimension of the patient. Often, however, the patient is not aligned perfectly at isocenter, so the off-center positioning needs to be accounted for in the calculation of lateral dimension. According to Siemens' patents, off-center patient positioning is explicitly accounted for in the calculation of lateral extent.[22] First, an offset correction factor quantifying the distance the table is from isocenter was calculated. The vertical position of the table at isocenter is hard coded into the CT scanner, so the scanner can readily determine the table-to-isocenter distance. In this investigation, the offset correction factor for any given patient was not explicitly known, but was calculated from the axial images by measuring the distance from the center of the image to the center of the table. Once the offset correction factor was calculated, the lateral dimension at the offset table height at each table position, i, was defined as:

$$LAT(i)_{offset} = \frac{SID + OCF - \left(\frac{1}{2} \times AP(i)\right)}{SID} \times LAT(i)_{iso} \tag{4}$$

where OCF is the offset correction factor. LAT_{offset} is the LAT dimension of patient size. Figure 3 provides a diagram of the scanner geometry with all components of Eq. 4 labeled.

2.C. Estimating tube current modulation schemes from attenuation data

2.C.1. Longitudinal modulation

In the Siemens' AEC algorithm (CARE Dose4D, Siemens Healthineers, Forchheim, Germany), tube current is first determined on the basis of the topogram by comparing the actual patient attenuation to reference patient attenuation values.[17,23] While both AP and LAT water-equivalent estimates of patient size can be extracted from a measured or simulated topogram, longitudinal modulation works on the basis of the maximum attenuation at each table position, regardless of whether it occurred in the AP or LAT direction. The maximum attenuation at each table position, i, calculated from the size data in the topogram is defined as:

$$A_{\max}(i) = \max\left(\exp\left(\mu_{water,E} \times AP(i)\right), \exp\left(\mu_{water,E} \times LAT(i)\right)\right) \tag{5}$$

Figure 4 (left) shows the maximum attenuation calculated from the AP and LAT size data previously shown.

After the maximum attenuation at each table position was calculated, tube current values corresponding to those attenuation values were determined. Tube current (mA) at each table position, i, calculated from the corresponding patient attenuation was defined as:

$$mA(i) = \frac{QRM \times pitch}{t} \times \left(\frac{A_{\max}(i)}{A_{ref}}\right)^{b} \tag{6}$$

where QRM is the quality reference effective tube current-time product (effective mAs) set directly on the scanner by the user, t is the gantry rotation time, $A_{\max}$ is the patient attenuation determined using Eq. 5, A_{ref} is the protocol-specific reference attenuation hard coded into the CARE Dose4D algorithm and b is a strength parameter that can be set according to individual preferences for the tube current increase and decrease. The QRM represents the effective mAs (mAs/pitch) value selected by the user to produce the desired image quality for a standard-sized patient, and A_{ref} represents the standard-sized patient attenuation for which the QRM is specified.[17] The default strength parameter setting on all Siemens CT scanners (including all scanners used in this investigation) is "Average." For the "Average" strength, b is 0.33 for attenuation greater than A_{ref} and 0.5 for attenuation less than A_{ref}.[17,24] For pediatric chest and abdomen/pelvis scans acquired at 80 kV, the strength parameter necessary to achieve agreement between estimated and actual tube current values was empirically determined to be 0.4 for attenuation greater than A_{ref} and 0.65 for attenuation less than A_{ref}.

Applying Eq. 6 to the patient attenuation determined at each table position in the topogram yielded an estimate of the

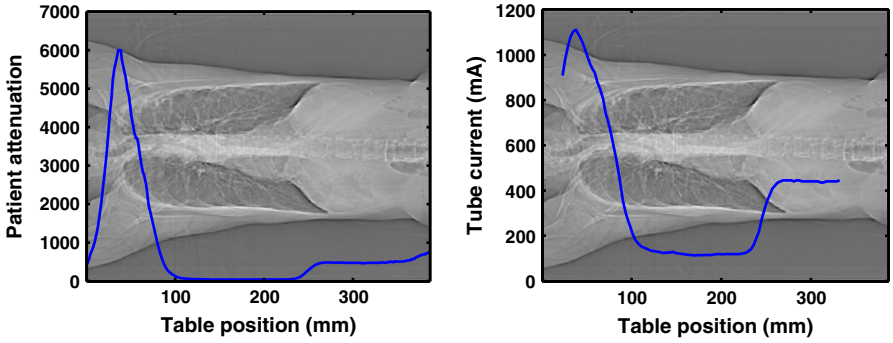

FIG. 4. (Left) Maximum patient attenuation at each table position calculated from patient size data using Eq. 5. (Right) Tube current profile calculated from patient attenuation data using Eq. 6 at all table positions with corresponding axial CT images. [Color figure can be viewed at wileyonlinelibrary.com]

maximum tube current at each table position. This relationship between tube current and table position is called the "control curve" and represents modulation of the tube current along the length of the patient. Figure 4 shows the control curve (right) calculated from the attenuation profile (left) of an adult patient. Because the topogram image is used to localize the anatomy that is to be scanned, the boundaries of the topogram image often extend longitudinally beyond those of the CT image data. As such, the control curve in Fig. 4 shows tube current as a function of table position only for positions where there were corresponding axial CT images.

2.C.2. Angular modulation

In addition to adapting the tube current to patient size and modulating it along the length of the patient according to the attenuation data from the topogram, the CARE Dose4D algorithm also modulates the tube current angularly according to on-line (i.e., real-time) angular attenuation measurements (i.e., angular modulation).[23] This technique requires that patient attenuation is constantly measured as the tube rotates about the patient during the scan acquisition.[23] To set tube current values in response to angular attenuation, an extrapolation method is implemented for computing an attenuation profile for the next half rotation based on the measured angular attenuation profile for the previous half rotation.[25] The extrapolation method assumes that the angular attenuation profile of the next half rotation very closely matches the angular attenuation profile measured in the previous half rotation. For any given Siemens CT scanner, the maximum distance between adjacent half rotations is on the order of a few centimeters, so this assumption is expected to be relatively robust.

In this work, the only patient attenuation data used were the attenuation data derived from the actual or simulated topogram. In order to model on-line angular modulation, patient attenuation at each gantry angle is necessary. Taking advantage of the fact that AP attenuation is measured at tube angles of 0° and 180° and LAT attenuation is measured at tube angles of 90° and 270°, patient attenuation at any tube angle was estimated using the AP and LAT patient attenuation profiles extracted from the topogram. For a given starting table position and starting tube angle of a CT scan, the tube angle at any table position, TP, is defined as:

$$\theta(TP) = \frac{360^\circ}{NC \times Pitch} \times (TP - TP_0) + \theta_0 \quad (7)$$

where NC is the nominal collimation of the beam, TP_0 is the table position and θ_0 is the tube angle where the x-ray beam turns on respectively. The table positions at which the tube angle is in the AP (0° and 180°) and LAT (90° and 270°) locations were determined. Patient attenuation from the AP and LAT attenuation profiles at those respective table positions was then used to interpolate patient attenuation at any table position across the scan length (i.e., any tube angle). Interpolation was performed using a piecewise cubic Hermite interpolating polynomial.[26] Figure 5 (left) shows the angular attenuation profile as a function of table position that is calculated from the AP and LAT size data.

Using the extrapolated attenuation data, angular modulation at a table position, i, is defined as:

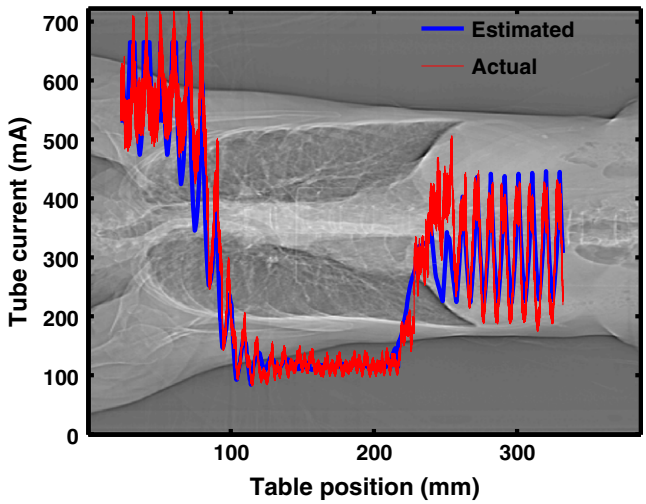

FIG. 6. Actual and estimated tube current values of adult chest patient. Estimated tube current values calculated from control curve and angular modulation scheme from Figs. 4 and 5, respectively. [Color figure can be viewed at wileyonlinelibrary.com]

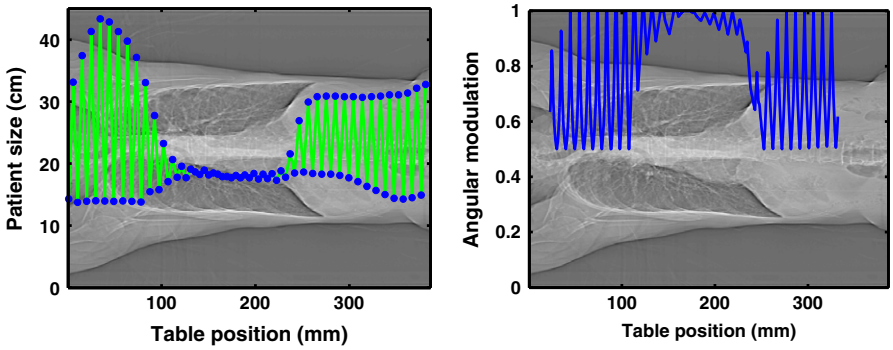

FIG. 5. (Left) Angular attenuation profile determined from patient size data extracted from topogram. (Right) Angular modulation scheme calculated from angular attenuation data using Eq. 8 at all table positions with corresponding axial CT images. [Color figure can be viewed at wileyonlinelibrary.com]

$$m(i) = 1 - \mu(i) \times \frac{A_{\max}^{q} - A(i - hROT)^{q}}{A_{\max}^{q} - A_{\min}^{q}} \quad (8)$$

where $hROT$ is the half rotation of the tube equal to $(NC/2) \times pitch$, $A(i - hROT)$ is the patient attenuation at the table position a half rotation prior to the current table position, $A_{\min}$ is minimum patient attenuation over the previous half rotation, $A_{\max}$ is the maximum patient attenuation over the previous half rotation, q is an optimization parameter between 0.5 and 1.0 and $\mu(i)$ is a gantry rotation time-dependent parameter that limits the amount of modulation allowed at a given table position.[25] If there are no attenuation data available in the previous half rotation, the angular modulation is set to 1 (i.e., no modulation). Figure 5 shows the angular modulation scheme (right) determined from the angular attenuation profile (left) of the adult chest patient. This figure specifically illustrates that in the lung (e.g., table position approximately 200) that there is little difference between the $A_{\max}$ and $A_{\min}$ values and therefore little angular modulation. The figure also illustrates that in the lung apices/shoulder region that there is a large difference between these two attenuation values and therefore more modulation, which is limited by parameter q and rotation time constraints.

2.C.3. Combining longitudinal and angular modulation

Putting it all together, the control curve from Section 2.C.1 and the angular modulation scheme from Section 2.C.2 were combined to generate an estimated tube current profile. For the estimated tube current, the tube current at each table position, i, is defined as:

$$mA(i)_{AEC} = mA(i)_{control} \times m(i) \quad (9)$$

where $mA(i)_{control}$ is the maximum tube current at the table position calculated using Eq. 6 and $m(i)$ is the angular modulation at the table position calculated using Eq. 8. CT scanners have operating limits for tube current values that vary as a function of tube potential.[27] At 120 kV, the tube potential at which the images of the example adult chest patient were acquired, the maximum tube current is 665 mA. Applying the appropriate tube limits to the tube current profile calculated using Eq. 9, a final estimated tube current profile is calculated. Figure 6 shows the actual and estimated tube current values for the example patient. Figure 7 shows the general workflow for the various methods to obtain Siemens AEC schemes.

2.D. Validation – comparing estimated and actual tube current values in a patient cohort

The methods to estimate Siemens tube current values described above were applied to a set of pediatric and adult patients who underwent clinically indicated chest (n = 20) and abdomen/pelvis (n = 20) CT examinations.[28] For each patient, the measured topogram, axial images, and projection data were all acquired with IRB approval. Axial images were reconstructed at full 500 mm field of view (to avoid having any anatomy outside of the image). Table I outlines the characteristics of the patients used in the validation. All patients were scanned on a Sensation 64 CT scanner, and a variety of scan techniques were used. Water equivalent diameters (WED) calculated from the central slice of the axial images using the equations outlined in AAPM Report 220 ranged

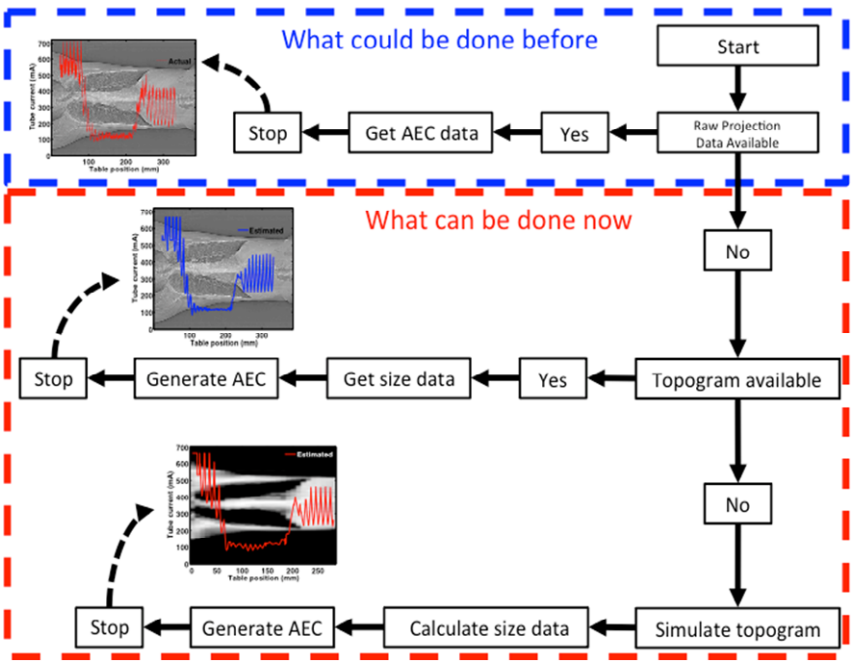

FIG. 7. Workflow of available methods to generate Siemens AEC schemes. This investigation introduces methods to estimate AEC schemes using patient size calculated from either an actual or simulated topogram. [Color figure can be viewed at wileyonlinelibrary.com]

TABLE I. Patient size and scan techniques for validation patients.

		Patient	WED (cm)	Collimation (mm)	kV	Pitch	Rotation time (s)	QRM
Chest	Pediatric	1	21.70	28.8	120	1	0.5	55
		2	18.69	28.8	100	1	0.5	55
		3	18.29	19.2	100	1	0.5	55
		4	15.40	28.8	100	1	0.5	55
		5	12.59	28.8	80	1	0.5	55
		6	22.99	19.2	100	1	0.5	55
		7	19.36	28.8	100	1	0.5	55
		8	26.49	19.2	100	1	0.5	55
		9	19.98	28.8	100	1	0.5	55
		10	22.84	19.2	100	1	0.5	55
	Adult	1	24.74	19.2	120	1	0.5	250
		2	18.35	19.2	120	1	0.5	250
		3	20.89	19.2	120	1	0.5	250
		4	22.36	19.2	120	1	0.5	250
		5	19.34	19.2	120	1	0.5	250
		6	25.25	19.2	120	1	0.5	250
		7	13.97	19.2	120	1	0.5	250
		8	16.96	19.2	120	1	0.5	250
		9	20.48	19.2	120	1	0.5	250
		10	34.76	19.2	120	1	0.5	250
Abdomen/pelvis	Pediatric	1	23.73	28.8	100	1	0.5	65
		2	20.1	28.8	80	1	0.5	55
		3	24.06	28.8	120	1	0.5	65
		4	20.69	28.8	100	1	0.5	65
		5	21.59	28.8	120	1	0.5	65
		6	19.66	28.8	100	1	0.5	65
		7	24.32	28.8	100	1	0.5	65
		8	22.83	28.8	100	1	0.5	35
		9	21.34	28.8	100	1	0.5	65
		10	14.11	28.8	80	1	0.5	55
	Adult	1	27.78	19.2	120	0.95	0.5	275
		2	19.97	19.2	120	1	0.5	275
		3	33.69	19.2	120	0.45	0.5	275
		4	24.57	19.2	120	1	0.5	275
		5	38.40	19.2	120	0.8	1.0	275
		6	23.87	19.2	120	1	0.5	275
		7	26.08	19.2	120	0.95	0.5	275
		8	30.77	19.2	120	1	0.5	275
		9	28.02	19.2	120	1	0.5	275
		10	37.34	19.2	120	0.75	0.5	275

WED, water equivalent diameter; QRM, quality reference effective mAs.

from 12.59 to 34.76 cm for patients who underwent chest scans and 14.11 to 38.4 cm for patients who underwent abdomen/pelvis scans.[19] It should be noted that it is our clinical practice to vary the kV for different sized pediatric patients. It should also be noted that for this scanner, different reference sizes (different attenuation reference values) are used for pediatric and adult patients; for later scanners Siemens uses a single set of reference attenuation values for adult and pediatric patients. For abdomen/pelvis scans, different pitch values are used, usually for larger patients. This is because Siemens scanners use the effective mAs concept (effective mAs = mAs/pitch) and automatically adjust the tube current to changes in pitch. For larger patients, a higher effective mAs value is desired to maintain image quality; this results in higher mA values being required and often results in the tube current reaching the tube limit. To overcome this, lower pitch values – and therefore lower mA values – are used to maintain the desired effective mAs. These are reflected in Table I.

Models of patient anatomy were created from the image data and used as the patient geometry in the patient attenuation simulations described in Section 2.B.1. AP and LAT patient dimensions were determined from the measured and simulated topograms for each patient and then used as the inputs to the methods to estimate Siemens tube current values.

For each chest scan, the lungs and breasts (if female) were segmented from the axial images. For the abdomen/pelvis scans, the liver, spleen, and kidneys were segmented from the images.[28] For each patient, the actual tube current values were then extracted from the projection data. Organ doses were estimated with detailed Monte Carlo simulations using both the estimated and actual tube current values.[20,29] The estimated tube current values were validated against the actual tube current values for each patient by comparing both average tube current and organ dose estimates.

3. RESULTS

To illustrate the agreement between actual and estimated patient dimensions derived from actual and simulated topograms, respectively, Fig. 8 shows AP and LAT patient dimensions estimated from the simulated topogram compared with AP and LAT patient dimensions extracted from the actual topogram for patients who underwent clinically indicated chest (left) and abdomen/pelvis (right) scans. To illustrate the prediction of tube current values based on these patient dimension estimates, Fig. 9 use the same patients from Fig. 8 to show the tube current values estimated from the AP and LAT dimensions derived from those simulated topograms compared with actual tube current values extracted from the original projection data.

A comparison of the average tube current from estimated and actual tube current values for all patients is tabulated in Table II. Across all patients, the average error for tube current values estimated from patient data extracted from the actual topogram (actual topo) was 3.9%. For tube current values estimated from patient attenuation determined from a simulated topogram (sim topo), the average error was 5.8%.

Table III shows a comparison of lung and breast dose estimates from Monte Carlo simulations of chest CT exams using actual and estimated tube current values. Estimated tube current values were derived from patient attenuation data from the actual topogram (actual topo) and a simulated topogram that matches the topogram that would have been acquired on the Siemens scanner (sim topo). The average error for lung and breast dose ranged from 3.4% to 6.6%. Table IV shows a

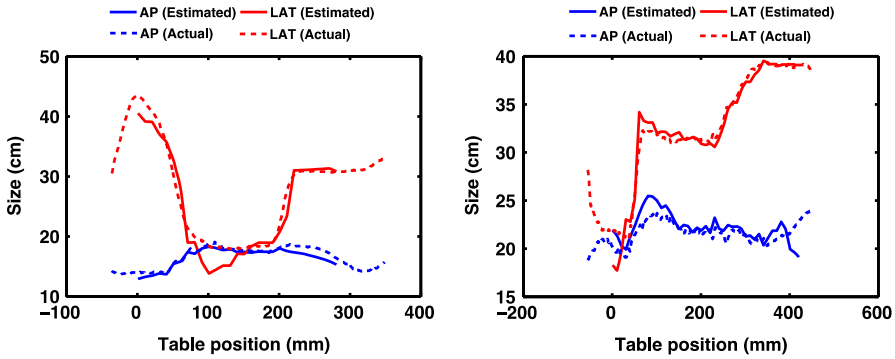

FIG. 8. (Left) Estimated AP and LAT patient dimensions compared with AP and LAT dimensions of patient size extracted from the measured topogram of a patient who underwent a clinically indicated chest CT exam (Patient Chest Adult 7 from Table I). (Right) Estimated AP and LAT patient dimensions compared with AP and LAT patient dimensions size extracted from the measured topogram of a patient who underwent a clinically indicated abdomen/pelvis CT exam (Patient Abdomen/Pelvis Adult 4 from Table I). [Note: The estimated patient attenuation data (solid lines) was derived from the patient's axial image data and therefore does not include the extra anatomy before and after the scan range in the patient's actual topogram (dashed lines).] [Color figure can be viewed at wileyonlinelibrary.com]

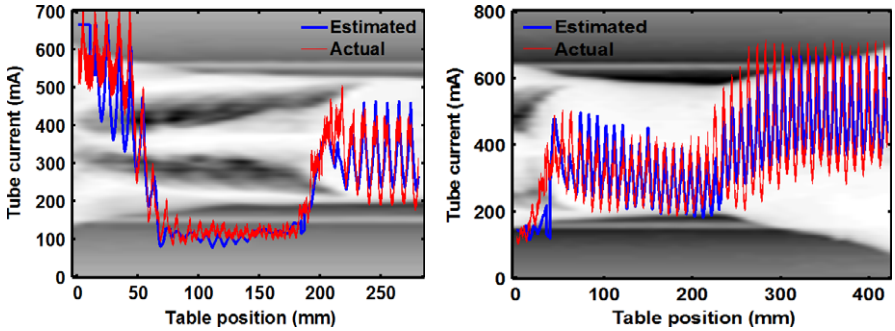

FIG. 9. (Left) Tube current values from simulated topogram and actual tube current values for chest patient (Patient Chest Adult 7 from Table I). (Right) Tube current values from simulated topogram and actual tube current values scheme for abdomen/pelvis patient (Patient Abdomen/Pelvis Adult 4 from Table I). [Color figure can be viewed at wileyonlinelibrary.com]

TABLE II. Comparison of average tube current between actual and estimated tube current values.

			Average mA				
		Patient	Actual	Estimated (Actual topo)	% error	Estimated (Sim topo)	% error
Chest	Pediatric	1	329.2	319.0	3.1	321.7	2.3
		2	224.4	222.0	1.1	201.2	10.3
		3	257.1	230.2	10.5	227.8	11.4
		4	153.3	135.3	11.7	134.7	12.1
		5	141.6	140.0	1.1	147.6	4.2
		6	321.9	308.3	4.2	309.0	4.0
		7	296.6	273.1	7.9	265.8	10.4
		8	370.8	351.9	5.1	338.6	8.7
		9	311.3	308.0	1.1	314.5	1.0
		10	289.2	275.8	4.6	283.5	2.0
	Adult	1	418.3	401.3	4.1	360.5	13.8
		2	365.4	361.8	1.0	395.6	8.3
		3	433.3	417.8	3.6	384.4	11.3
		4	471.5	467.4	0.9	428.4	9.1
		5	381.9	383.7	0.5	361.1	5.5
		6	513.7	485.7	5.5	526.9	2.6
		7	285.5	273.7	4.1	287.3	0.6
		8	330.8	328.0	0.9	338.9	2.5
		9	381.9	377.2	1.2	363.5	4.8
		10	567.2	547.1	3.5	588.4	3.7
Abdomen/pelvis	Pediatric	1	327.0	353.0	8.0	338.5	3.5
		2	275.9	268.7	2.6	290.4	5.3
		3	290.9	277.6	4.6	268.7	7.6
		4	253.0	274.4	8.5	274.7	8.6
		5	285.2	278.8	2.2	262.9	7.8
		6	251.2	270.6	7.7	259.8	3.4
		7	259.3	261.3	0.8	240.4	7.3
		8	129.6	138.6	6.9	128.5	0.9
		9	227.0	227.9	0.4	235.4	3.7
		10	185.5	182.4	1.7	175.0	5.7
	Adult	1	463.5	474.6	2.4	502.6	8.4
		2	301.8	322.2	6.8	337.1	11.7
		3	323.7	345.0	6.6	329.2	1.7
		4	357.7	378.5	5.8	378.5	5.8
		5	392.2	400.5	2.1	402.1	2.5
		6	418.8	439.7	5.0	405.8	3.1
		7	473.9	471.7	0.5	461.3	2.7
		8	470.5	463.9	1.4	452.8	3.8
		9	450.4	446.5	0.9	414.1	8.1
		10	334.4	358.1	7.1	337.7	1.0
		Average % error			3.9		5.8
		Standard deviation			3.0		3.7

comparison of liver, kidney, and spleen dose estimates from Monte Carlo simulations of abdomen/pelvis CT exams using actual and estimated tube current values. The average error for liver, kidney, and spleen dose ranged from 4.2% to 5.3%.

4. DISCUSSION AND CONCLUSIONS

In this study, methods were developed to: (a) estimate patient attenuation information based on a simulated CT localizer radiograph (e.g., topogram), which matched the attenuation data that would have been determined by the scanner and could be applied to any voxelized patient model and (b) estimate the tube current values based on size information extracted from either a measured or simulated CT localizer radiograph. The tube current estimates were shown to take into account many practical factors such as patient attenuation information, scanner limits, and image quality reference factor (such as Quality Reference mAs). Each

TABLE III. Comparison of lung and breast dose from Monte Carlo simulations of chest CT exams using actual tube current values and tube current values estimated from actual topograms (actual topo) and simulated topograms (sim topo).

			Lung (mGy)					Breast (mGy)				
		Patient	Actual	Estimated (Actual topo)	% error	Estimated (Sim topo)	% error	Actual	Estimated (Actual topo)	% error	Estimated (Sim topo)	% error
Chest	Pediatric	1	13.37	12.65	5.4	13.53	1.2	–	–	–	–	–
		2	5.57	5.36	3.8	4.91	11.9	–	–	–	–	–
		3	7.23	6.51	10.0	6.39	11.6	–	–	–	–	–
		4	5.06	4.33	14.4	4.21	16.9	–	–	–	–	–
		5	2.67	2.60	2.6	2.74	2.8	–	–	–	–	–
		6	9.18	8.85	3.6	8.54	7.0	7.60	7.40	2.6	7.70	1.3
		7	8.84	8.13	8.0	7.96	9.9	7.28	6.76	7.1	6.87	5.6
		8	9.66	9.05	6.3	8.89	8.0	8.36	7.87	5.9	7.79	6.8
		9	8.16	7.84	3.9	7.98	2.2	5.91	5.83	1.4	5.75	2.7
		10	9.00	8.33	7.4	9.20	2.2	6.10	5.76	5.6	5.77	5.4
	Adult	1	20.37	19.48	4.4	18.45	9.4	–	–	–	–	–
		2	18.10	18.09	0.1	19.78	9.3	–	–	–	–	–
		3	19.83	18.98	4.3	17.54	11.6	–	–	–	–	–
		4	21.33	20.96	1.7	19.56	8.3	–	–	–	–	–
		5	16.76	16.78	0.1	15.58	7.0	–	–	–	–	–
		6	24.62	23.15	6.0	24.94	1.3	22.83	21.40	6.3	24.52	7.4
		7	15.11	14.41	4.6	15.52	2.7	8.82	8.62	2.3	9.37	6.2
		8	16.06	15.96	0.6	16.56	3.1	10.60	10.60	0.1	11.09	4.6
		9	19.23	18.93	1.6	18.21	5.3	15.78	15.87	0.6	15.72	0.4
		10	18.67	18.13	2.9	18.46	1.1	17.43	17.09	2.0	18.19	4.4
Average % error					4.6		6.6			3.4		4.5
Standard deviation					3.5		4.5			2.6		2.3

method was evaluated by comparing estimated tube current values to actual tube current values directly and by comparing organ doses estimated from Monte Carlo simulations that incorporated each set of estimated tube current values. The results demonstrated excellent agreement and indicate that tube current values can be accurately estimated using the size data extracted from a measured or simulated topogram and the steps described in this work.

While some differences between the actual and estimated mA values are seen in some projections in several of the figures (Figs. 6 and 9), these variations did not result in large differences in average mA values or in organ dose estimates. Some differences were expected as this work describes an implementation of methods that are similar, but not identical, to the methods used by one manufacturer (Siemens). The resulting validation study demonstrated that these differences are small in terms of average mA and organ dose estimates; for the actual topo-based method 97% of organ doses were within 10% of the reference values and for the sim topo method, 93% of organ doses were within 10% as well. Future work will investigate methods to reduce these differences and their effects on average mA values and organ doses.

The wide varieties of scan techniques and patient sizes used in the validation study indicate that the methods developed to estimate tube current values are generalizable across different scan types and patient sizes. The methods to estimate Siemens tube current values may also be generalizable to Siemens scanners beyond the Sensation 64. Figure 10 shows estimated and actual tube current values for patients who underwent clinically indicated chest CT examinations on a Sensation 16 (left) and Definition Flash (right) scanner. All methodologies described in this investigation were applied in conjunction with scanner-specific machine limits to generate the estimated tube current values. This figure demonstrates excellent agreement between estimated and actual tube current values for both scanners. It should be noted, though, that parameters used to estimate tube current values might vary for other scanner models and possibly even different software releases on the same models.

Prior to this investigation, the only way to incorporate detailed tube current values into Monte Carlo simulations was to extract the actual tube current profile from the projection data. That method works well, but is limited by the fact that manufacturer tools are required to properly read the projection data and extract the relevant tube current information. It is also limited in that it can only be applied to patient datasets that have actually undergone a CT scan that used AEC. This investigation extends the ability to accurately estimate tube current values using patient size data determined from either an actual or a simulated topogram. Thus, tube current values can now be generated for any voxelized patient model, including reference voxelized phantoms in which a voxelized (or geometric) representation exists and from which a simulated topogram can be generated. This allows the estimation

TABLE IV. Comparison of liver, kidney and spleen dose from Monte Carlo simulations of abdomen/pelvis CT exams using actual tube current values and tube current values estimated from actual topograms (actual topo) and simulated topograms (sim topo).

			Liver (mGy)					Kidney (mGy)					Spleen (mGy)				
		Patient	Actual	Estimated (Actual topo)	% error	Estimated (Sim topo)	% error	Actual	Estimated (Actual topo)	% error	Estimated (Sim topo)	% error	Actual	Estimated (Actual topo)	% error	Estimated (Sim topo)	% error
Abdomen/pelvis	Pediatric	1	7.66	8.17	6.7	7.71	0.7	7.21	7.71	6.9	7.31	1.4	7.53	7.71	6.9	7.76	3.1
		2	3.53	3.41	3.4	3.76	6.5	3.31	3.20	3.3	3.46	4.5	3.06	3.20	3.3	3.27	6.9
		3	11.93	11.47	3.9	10.88	8.8	11.83	11.10	6.2	11.02	6.9	12.13	11.10	6.2	11.36	6.4
		4	5.78	6.16	6.6	6.22	7.6	6.80	7.25	6.6	7.43	9.3	4.76	7.25	6.6	5.13	7.8
		5	13.92	13.87	0.4	12.80	8.1	10.21	9.78	4.2	9.46	7.4	11.80	9.78	4.2	11.04	6.4
		6	6.13	6.62	8.0	6.27	2.3	6.16	6.63	7.6	6.38	3.6	5.98	6.63	7.6	6.07	1.5
		7	6.37	6.45	1.3	5.84	8.3	5.77	5.72	0.9	5.48	5.0	5.95	5.72	0.9	5.44	8.6
		8	3.40	3.60	5.9	3.44	1.2	3.06	3.22	5.2	3.02	1.3	2.93	3.22	5.2	2.86	2.4
		9	6.85	6.80	0.7	7.26	6.0	6.11	6.16	0.8	6.44	5.4	6.82	6.16	0.8	7.14	4.7
		10	2.73	2.72	0.4	2.49	8.8	2.68	2.65	1.1	2.55	4.9	2.88	2.65	1.1	2.70	6.3
	Adult	1	22.27	24.37	9.4	24.43	9.7	21.34	23.16	8.5	23.09	8.2	23.85	23.16	8.5	26.12	9.5
		2	15.22	14.78	2.9	16.63	9.3	13.43	13.24	1.4	14.77	10.0	12.83	13.24	1.4	14.11	10.0
		3	23.77	22.71	4.5	23.63	0.6	26.79	25.83	3.6	27.90	4.1	26.79	25.83	3.6	27.00	0.8
		4	17.39	19.20	10.4	18.07	3.9	16.76	18.10	8.0	17.63	5.2	14.97	18.10	8.0	15.92	6.4
		5	27.66	27.22	1.6	28.75	3.9	30.30	29.65	2.3	31.12	2.7	33.46	29.65	2.2	33.66	0.6
		6	16.64	18.15	9.1	16.03	3.7	15.09	16.34	8.3	14.44	4.3	15.40	16.34	8.3	14.72	4.4
		7	19.63	19.55	0.4	19.67	0.2	20.88	20.76	0.6	20.07	3.9	21.51	20.76	0.6	20.33	5.5
		8	19.48	20.98	7.7	18.83	3.3	19.28	20.55	6.6	18.39	4.6	19.18	20.55	6.6	18.42	4.0
		9	17.87	17.92	0.3	16.63	6.9	18.37	18.41	0.2	17.40	5.3	17.87	18.41	0.2	16.62	7.0
		10	25.01	24.93	0.3	25.77	3.0	25.46	24.61	3.3	26.37	3.6	28.41	24.61	3.3	29.36	3.3
Average % error					4.2		5.1			4.3		5.1			4.9		5.3
Standard deviation					3.5		3.2			2.9		2.3			2.8		2.8

4273

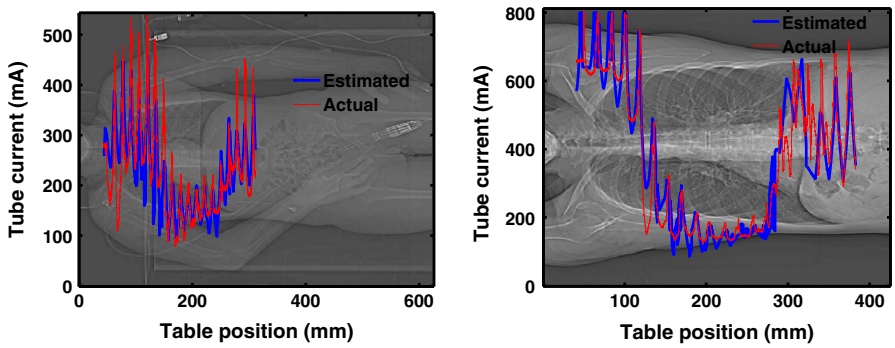

FIG. 10. Estimated and actual tube current values for a patient undergoing a chest scan on a Sensation 16 (left) and a separate patient undergoing a chest scan on a Definition Flash (right). For the Sensation 16 case, the error between the average tube current from the estimated and actual AEC scheme was 0.2%. For the Definition Flash case, the error between the average tube current from the estimated and actual AEC scheme was 0.8%. [Color figure can be viewed at wileyonlinelibrary.com]

of tube current values for any voxelized patient model, including reference voxelized phantoms that have all radiosensitive organs modeled and which will facilitate a more complete assessment of patient dose using these reference phantoms under simulated AEC scan conditions. This will also enable other analyses such as: (a) doses to fully-, partially- or indirectly irradiated organ doses from AEC CT exams and (b) investigations of the relationship between patient size and dose under AEC conditions to develop relationships such as those described in AAPM report 204 (Size Specific Dose Estimates), but for AEC conditions.

There are several limitations to this study. The methods to estimate the TCM scheme are particular to one manufacturer (Siemens). While a method to estimate TCM functions for all scanners is highly desirable, a single approach would be very difficult to achieve given the divergence of approaches and implementations that exist across manufacturers (a review of which is provided in ref. 1). For example, while all manufacturers base their TCM schemes on a measure of patient attenuation extracted from the CT localizer radiograph (i.e., topogram or scout), what those values represent (water equivalent attenuation[18] or square root of the projection area[30]) and whether these values are available to users or not (i.e., where they are stored and in what format) differ between manufacturers. It should be noted that in AAPM Task Group Report 220, the reporting of water equivalent attenuation values in the localizer radiograph was specifically identified as an acceptable method to provide attenuation values to users (Section 5 of ref. 19). In addition, how these attenuation values are used to create the TCM schemes also diverges substantially between manufacturers. This manuscript described one approach to model how Siemens CT scanners create the TCM function, while a previous study[30] describes some aspects of GE's tube current modulation scheme, including using beam attenuation from the CT localizer radiograph and "a set of empirically determined noise prediction coefficients." Therefore, development of a generalizable approach, and the validation of those generalized characterizations, remains the subject of future investigations.

Another limitation is that a limited set of parameters (kV, QRM, pitch, AEC strength, etc.) values were used in the validation study. Because the validation was based on actual patient scans, it was limited to the set of parameters we use clinically for pediatric and adult chest and abdomen/pelvis scans. In addition, a complete exploration of the parameter space is difficult and complex due to the interaction of some of the parameters. For example, Siemens scanners use the effective mAs concept (effective mAs = mAs/pitch) and therefore adjust tube current in response to changes in pitch. Thus, when pitch values are increased, mA values are increased accordingly and may result in reaching tube limits (which may vary from one model to another) at certain pitch values or when larger patients (requiring higher effective mAs values) are scanned. In Table I, some pitch values are reduced for larger patients so that a lower tube current value can be used to maintain the desired effective mAs. Thus, only a limited exploration of the parameter space was performed.

ACKNOWLEDGMENTS

This work was supported in part by a grant from the National Institute of Biomedical Imaging and Bioengineering of the National Institutes of Health under award number R01EB017095 and by a grant from Siemens Healthcare (now Siemens Healthineers) through a Master Research Agreement with UCLA Department of Radiological Sciences. The content is solely the responsibility of the authors and does not necessarily represent the official views of the National Institutes of Health. C.H.M. receives research support from Siemens Healthcare. M.M.G's department has a master research agreement with Siemens Healthcare.

[a]Author to whom correspondence should be addressed. Electronic mail: mmcnittgray@mednet.ucla.edu.

REFERENCES

1. McCollough CH, Bruesewitz MR, Kofler JM. CT dose reduction and dose management tools: overview of available options. *Radiographics*. 2006;26:503–512.
2. Kalra MK, Maher MM, Toth TL, et al. Techniques and applications of automatic tube current modulation for CT. *Radiology*. 2004;233:649–657.
3. Kalra MK, Maher MM, Toth TL, Kamath RS, Halpern EF, Sanini S. Comparison of z-axis automatic tube current modulation technique with

fixed tube current CT scanning of abdomen and pelvis. *Radiology*. 2004;232:347–353.
4. Angel E, Yaghmai N, Jude CM, et al. Monte Carlo simulations to assess the effects of tube current modulation on breast dose for multidetector CT. *Phys Med Biol*. 2009;54:497–512.
5. Angel E, Yaghmai N, Jude CM, et al. Dose to radiosensitive organs during routine chest CT: effects of tube current modulation. *Am J Roentgenol*. 2009;193:1340–1345.
6. Khatonabadi M, Zhang D, Mathieu K, et al. A comparison of methods to estimate organ doses in CT when utilizing approximations to the tube current modulation function. *Med Phys*. 2012;39:5212–28.
7. Petoussi-Henss N, Zankl M, Fill U, Regulla D. The GSF family of voxel phantoms. *Phys Med Biol*. 2002;47:89–106.
8. International Commission on Radiological Protection, Adult Reference Computation Phantoms, ICRP Publication 110; 2009.
9. American Association of Physicists in Medicine, Size-Specific Dose Estimates (SSDE) in Pediatric and Adult Body CT Examinations, AAPM Report 204; 2011.
10. Gies M, Kalender WA, Wolf H, Suess C. Dose reduction in CT by anatomically adapted tube current modulation. I. Simulation studies. *Med Phys*. 1999;26:2235–2247.
11. Kalender WA, Wolf H, Suess C. Dose reduction in CT by anatomically adapted tube current modulation. II. Phantom measurements. *Med Phys*. 1999;26:2248–2253.
12. Schlattl H, Zankl M, Becker J, Hoeschen C. Dose conversion coefficients for CT examinations of adults with automatic tube current modulation. *Phys Med Biol*. 2010;55:6243–6261.
13. Schattl H, Zankl M, Becker J, Hoeschen C. Dose conversion coefficient for pediatric CT examinations with automatic tube current modulation. *Phys Med Biol*. 2012;57:6309–6326.
14. Li X, Segars WP, Samei E. The impact on CT dose of the variability in tube current modulation technology: a theoretical investigation. *Phys Med Biol*. 2014;58:4525–4548.
15. Tian X, Li X, Segars WP, Frush DP, Samei E. Prospective estimation of organ dose in CT under tube current modulation. *Med Phys*. 2015; 42:1575–1585.
16. Keat N. CT scanner automatic exposure control systems. MHRA Report 05016; 2005.
17. Favazza CP, Yu L, Leng S, Kofler JM, McCollough CH. Automatic exposure control systems designed to maintain constant image noise: effects on computed tomography dose and noise relative to clinically accepted technique charts. *J Comput Assist Tomogr*. 2015;39:437–442.
18. McMillan K, Bostani M, McCollough C, McNitt-Gray M. Calculating SSDE from CT exams using size data available in the DICOM header of CT localizer radiographs. *Med Phys*. 2014;41:423.
19. American Association of Physicists in Medicine. Use of Water Equivalent Diameter for Calculating Patient Size and Size-Specific Dose Estimates (SSDE) in CT. AAPM Report 220; 2014.
20. Turner AC, Zhang D, Kim HJ, et al. A method to generate equivalent energy spectra and filtration models based on measurements for multidetector CT Monte Carlo doseimetry simulations. *Med Phys*. 2009; 36:2154–2164.
21. Wolf H, Sub C, Popescu S. US Patent No. 20050058249 A1. U.S. Patent and Trademark Office; 2005.
22. Raupach R, Schaller A, Suss C, Wolf H. US Patent No. 7289595 B2. U.S. Patent and Trademark Office; 2007.
23. Flohr T. *CARE Dose4D White Paper*. Siemens Medical Solutions; 2011. Accessed https://static.healthcare.siemens.com/siemens_hwem-hwem_ssxa_websites-context-root/wcm/idc/groups/public/@us/@imaging/documents/download/mdaw/ndq2/~edisp/low_dose_care_dose_4d-00308408.pdf
24. Mahesh M, Physics MDCT. *The Basics: Technology, Image Quality and Radiation Dose*. Philadelphia: Lippincott, Williams and Wilkins; 2009.
25. Popescu S, Hentschel D, Strauss K, Wolf H. US Patent No. 5867555 A. U.S. Patent and Trademark Office; 1999.
26. Fritsch FN, Carlson RE. Monotone piecewise cubic interpolation. *SIAM J Numer Anal*. 1980;17:238–246.
27. Centre for Evidence-based Purchasing (CEP). 64 slice CT scanners technical specifications: Comparative specifications. CEP 08027; 2009.
28. Bostani M, McMillan K, Lu P, et al. Attenuation-based size metric for estimating organ dose to patients undergoing tube current modulated CT exams. *Med Phys*. 2015;42:958–968.
29. Bostani M, McMillan K, DeMarco JJ, Cagnon CH, McNitt-Gray MF. Validation of a Monte Carlo model used for simulating tube current modulation in computed tomography over a wide range of phantom conditions/challenges. *Med Phys*. 2014;41:112101.
30. Toth T, Ge Z, Daly MP. The influence of patient centering on CT dose and image noise. *Med Phys*. 2007;34:3093–4101.